Eur. Phys. J. D (2015) 69: 113
DOI: 10.1140/epjd/e2015-50893-1

THE EUROPEAN PHYSICAL JOURNAL D

Regular Article

Numerical simulation of dense cesium vapor emission and absorption spectra

Berislav Horvatić[a], Robert Beuc, and Mladen Movre

Institute of Physics, Bijenička cesta 46, 10000 Zagreb, Croatia

Received 17 December 2014 / Received in final form 12 March 2015
Published online 21 April 2015 –

Abstract. A recent ab initio calculation of Cs_2 electronic potential curves and electronic transition dipole moments provided us with an input for the numerical simulation of Cs_2 spectra. We investigated the red and near-infrared (600–1300 nm) absorption and emission spectrum of a dense cesium vapor for temperatures within the range 600–1500 K, using a novel time-efficient "semiquantum" approximation (SQA). Our study suggests that the SQA numerical simulation of the spectrum can be an efficient tool for the diagnostics of hot and dense dimer vapors. It also enables modelling of dense alkali vapor light sources.

1 Introduction

In a recent study [1] we introduced a time-efficient "semiquantum" approximation (SQA) for the theoretical simulation of the photoabsorption spectra of diatomic molecules. We dubbed this algorithm "semiquantum" because it makes use of fully quantum-mechanical (QM) expressions for energies, wave functions and transition dipole moment matrix elements, but the expression for the thermally averaged absorption coefficient is different from its truly quantum counterpart. The consumption of computer time with respect to the fully QM calculations is lower by up to four orders of magnitude, yet the results are more than satisfactory. We tested the SQA on the absorption spectra of potassium molecules, comparing its results to both the fully QM calculations [1] and the experimental data [2], and found a very good overall agreement. The agreement between the fully QM calculation and the SQA was additionally documented for four special cases of A-X, B-X, b-a, and c-a bands, covering the singlet-singlet as well as triplet-triplet transitions, situations with one, two or three Condon points, and illustrating the level of agreement for free-free, free-bound, and bound-bound types of transitions, respectively.

For heavier alkali-metal dimers the absorption spectrum is extremely dense due to the numerous vibrational levels populated in the ground state. Even the most powerful Doppler limited techniques are not able to fully resolve the rotational structure. It is only possible to resolve the structure of the sequences of the band spectrum (transitions with a fixed difference of the vibrational quantum numbers.) Also, and even more to the point here, when it comes to the accuracy of the SQA calculations, the extreme density of the Cs_2 spectrum is reasonably expected to promise even better results than those obtained for the much lighter potassium.

The alkali metals have been studied for many decades for their various interesting properties and applications [3], e.g. new light sources and thermoionic converters.

At the moment, the development of new light sources proceeds in two major directions: the semiconductor light emitting diode (LED and OLED) sources [4] and the high-intensity discharge (HID) sources [5]. Recent investigation has been focused on Na and Cs high-pressure discharge lamps [6].

A recent ab initio calculation of Cs_2 electronic potential curves and electronic transition dipole moments [7] provided us with a starting point for the numerical simulation of Cs_2 spectra. We investigated the red and near-infrared (600–1300 nm) absorption and emission spectrum of dense cesium vapor at high temperatures (600–1500 K). Our study shows that the SQA numerical simulation of the spectrum can be a very efficient tool for the diagnostics of hot and dense dimer vapors. It also enables modelling of dense alkali vapor light sources.

In Section 2 we first give a brief overview of the aspects of the theory of radiative transfer relevant for our study and do our best to define the physical quantities concerned (in view of the unfortunate diversity and vagueness of the inherited terminology.) In Section 2.1 we review (or, rather, just state) the procedure for calculating the thermally averaged reduced absorption coefficient in the SQA. In Section 2.2 we list the expressions relating the spectral radiance for the case of thermal emission to the reduced absorption coefficient, valid in the local thermodynamic equilibrium (LTE) approximation. In Section 3 we present the results for both the absorption and emission spectra. Section 4 comprises a brief summary of the results and a few comments on further prospects.

[a] e-mail: horvatic@ifs.hr

2 Theoretical background

The equation of radiative transfer along the line of sight in an absorbing and emitting medium reads [8]

$$\frac{dI_\nu}{ds} = j_\nu - \alpha_\nu I_\nu, \tag{1}$$

where I_ν is the "specific intensity", also termed "spectral radiance" (in units of erg s^{-1} sr^{-1} cm^{-2} Hz^{-1}), i.e. the radiant power per unit projected area, into a unit solid angle, within the frequency interval $[\nu, \nu + d\nu]$, j_ν is the volume emission coefficient (in units of erg s^{-1} sr^{-1} cm^{-3} Hz^{-1}), α_ν is the volume extinction coefficient (in units of cm^{-1}), and s is the geometric path along the ray.

The physics of equation (1) is mainly contained in the definitions of the extinction and emission coefficients. Once the extinction and emission coefficients of the excited gas are specified as functions of frequency and position, the equation of transfer may in principle be solved to obtain the intensity at any point. In order to keep the treatment as simple as possible, from now on, the subtleties involved in a general treatment of radiative transfer will be ignored. They would merely divert us from our primary goal of presenting the novel time-efficient approach. We treat the radiative transfer for a simple planar geometry only and assume the validity of the LTE approximation. The translational velocity distributions of the particles are then determined by Maxwellian distribution functions, the distribution of atoms, molecules and ions over their various excited states is given by the Boltzmann distribution law, and the relation between the number densities of the subsequent ionic states is given by the Saha equation. We also neglect the scattering contribution to the extinction coefficient, that is, the extinction coefficient is assumed to be due to absorption only, comprising the true absorption as well as the induced (stimulated) emission (treated as negative absorption). Furthermore, the emission and absorption coefficients are connected via Kirchhoff's relation for thermal radiation, $j_\nu = \alpha_\nu B_\nu(T)$, where $B_\nu(T)$ is the spectral radiance of the blackbody at temperature T,

$$B_\nu(T) = \frac{2h\nu^3}{c^2}\frac{1}{\exp(h\nu/k_BT) - 1}. \tag{2}$$

The general solution of the radiative transfer equation (1) is given by

$$I_\nu(L) = I_\nu(0)e^{-\tau_\nu(L)} + \int_0^{\tau_\nu(L)} d\tau' \, (j_\nu/\alpha_\nu)e^{-\left[\tau_\nu(L)-\tau'\right]}, \tag{3}$$

where L is the path length, $\tau_\nu(L)$ the optical depth, defined as:

$$\tau_\nu(L) = \int_0^L ds\alpha_\nu(s), \tag{4}$$

and the ratio j_ν/α_ν is termed the source function [9]. The first term in equation (3) describes the attenuation of the intensity of incoming radiation (from an external source) – the Lambert-Beer law – while the second term accounts for the final output of the emission of radiation from and reabsorption by the local sources. In the LTE approximation, which we use in this study, the source function reduces to $j_\nu/\alpha_\nu = B_\nu(T)$. Note that one can still have $T = T(s)$, so $B_\nu(T)$ need not be constant along the line of sight.

What actually gets observed and measured is the spectral radiation flux, a quantity of interest for studying lamps, outer mantles of "cold" stars, and planetary atmospheres, which depends both on the geometry of the source as well as on the configuration of the observing setup [10]. Obtaining it from $I_\nu(L)$ presents a problem of its own, which can be rather demanding as such, but this is not our subject here, so we restrict our considerations to the simplest geometry, a straight gas column of length L. This simple case is, however, not quite "purely academic", as it can be realized and is actually used in laboratory conditions, like e.g. in reference [11].

For an isothermal (but not necessarily homogeneous) gas column of length L the general solution (3) simplifies to

$$I_\nu(L) = I_\nu(0)e^{-\tau_\nu(L)} + B_\nu(T)\left[1 - e^{-\tau_\nu(L)}\right]. \tag{5}$$

If the gas column is homogeneous as well, that is, if $\alpha_\nu(s) = \text{const.} \equiv \alpha_\nu$, then $\tau_\nu(L) = \alpha_\nu L$.

In high-resolution line-by-line models the absorption coefficient of a molecule is given by the superposition of many lines i with the center position ν_i, determined from the energy difference between the upper (u) and lower (l) levels involved in the transition. The line absorption coefficient is

$$\alpha_\nu = k_\nu\left(1 - \frac{N_u}{N_l}\frac{g_l}{g_u}\right) \cong k_\nu\left(1 - e^{-h\nu_i/k_BT}\right), \tag{6}$$

where k_ν denotes the true absorption coefficient and the expression in the parentheses corrects for the stimulated emission. $N_l(N_u)$ and g_l (g_u) are the number densities and statistical weights in the lower (upper) state, respectively. The first equality in equation (6) is valid quite generally, while the second one holds only in LTE. If one has $h\nu/k_BT \gg 1$ within the spectral range considered, the stimulated emission may be neglected, $\alpha_\nu = k_\nu$, and the Planck distribution function $B_\nu(T)$ may be substituted by the Wien's approximate form $(2h\nu^3/c^2)\exp(-h\nu/k_BT)$.

The line absorption coefficient is usually expressed as a product of the number density of the absorbing particles (homonuclear diatomic molecules in our case) N_m and the (thermally averaged) absorption cross section σ_ν, as $k_\nu = N_m\sigma_\nu$. The molecular number density can be expressed in terms of the atomic density squared and the chemical equilibrium constant. In the present study we use the atomic-density-independent ("reduced") absorption coefficient $k_\nu/N_a^2 \equiv \kappa_\nu$, where N_a is the atomic number density. (For *heteronuclear* diatomic molecules AB, the reduced absorption coefficient is defined as $\kappa_\nu \equiv k_\nu/(N_\mathrm{A}N_\mathrm{B})$, where N_A and N_B are the number densities of atoms A and B, respectively.)

2.1 Thermally averaged reduced absorption coefficient

The line-by-line calculation of the molecular absorption coefficient is generally the most time-consuming part of a high-resolution radiative transfer computation. In the SQA the thermally averaged reduced absorption coefficient for the transition between two electronic states of a diatomic molecule reads [1]

$$\kappa_{\Lambda'',\Lambda'}(\nu,T) = C_{\Lambda'',\Lambda'}(\nu,T)\frac{2\mu k_B T}{\hbar^2} \times \sum_{v'',v'} \exp\left(-\tfrac{E_{v'',0,\Lambda''}}{k_B T}\right) \times \left|\langle \Phi_{v'',0,\Lambda''}\left|RD(R)\right|\Phi_{v',0,\Lambda'}\rangle\right|^2 \delta(\nu-\nu_{tr}), \quad (7)$$

where the first factor

$$C_{\Lambda'',\Lambda'}(\nu,T) = w\tfrac{8\pi^3\nu}{3hc}\left(\tfrac{h^2}{2\pi\mu k_B T}\right)^{3/2} \times \tfrac{\left(2-\delta_{0,\Lambda'+\Lambda''}\right)}{\left(2-\delta_{0,\Lambda''}\right)}\tfrac{2S+1}{(2S_a+1)(2S_b+1)} \quad (8)$$

comprises all the statistical factors pertaining to atomic and molecular electron states, including various partition functions. Here ν is the frequency of the absorbed photon, T is the temperature, Λ'' and Λ' label the lower and the upper electronic molecular state, respectively (Λ being the axial component of the electronic angular momentum), v is the vibrational quantum number and J the rotational quantum number, $\Phi_{v,J,\Lambda}$ is the radial wave function, and $D(R)$ the electronic transition dipole moment. The eigenenergies $E_{v,J,\Lambda}$ are measured from their respective dissociation limits E^{∞}_{Λ}, so the transition energy is given by $h\nu_{tr} = h\nu_0 + (E_{v',0,\Lambda'} - E_{v'',0,\Lambda''})$, where $h\nu_0 = E^{\infty}_{\Lambda'} - E^{\infty}_{\Lambda''}$. Finally, S_a (S_b) and S are the atomic and molecular spin quantum numbers, respectively, and $w = 1$ or $1/2$ for heteronuclear or homonuclear dimers, respectively. Expression (7) can be rewritten more compactly as

$$\kappa_{\Lambda'',\Lambda'}(\nu,T) = \frac{1}{\sqrt{k_B T}} \times \sum_{v'',v'} \exp\left(-\tfrac{E_{v'',0,\Lambda''}}{k_B T}\right) \mathrm{A}^{v'',v'}_{\Lambda'',\Lambda'}\delta(\nu-\nu_{tr}), \quad (9)$$

where

$$\mathrm{A}^{v'',v'}_{\Lambda'',\Lambda'} = w\tfrac{16\pi^3\sqrt{2\pi}}{3c\sqrt{\mu}}\tfrac{\left(2-\delta_{0,\Lambda'+\Lambda''}\right)}{\left(2-\delta_{0,\Lambda''}\right)}\tfrac{2S+1}{(2S_a+1)(2S_b+1)}\nu_{tr} \times \left|\langle \Phi_{v'',0,\Lambda''}\left|RD(R)\right|\Phi_{v',0,\Lambda'}\rangle\right|^2. \quad (10)$$

We analyzed the Cs_2 spectrum in the wavelength region of 600–1300 nm, where as many as 11 singlet and 19 triplet electronic transitions $\Lambda'' \to \Lambda'$ contribute to the absorption spectrum, and the total reduced absorption coefficient is the sum over all thirty of them,

$$\kappa_{tot}(\nu,T) = \frac{1}{\sqrt{k_B T}}\sum_{n=1}^{30}\kappa^{(n)}_{\Lambda'',\Lambda'}(\nu,T), \quad (11)$$

where the index n labels pairs of the contributing *electronic* states.

Disregarding which of the optical transitions $(v'',\Lambda'') \to (v',\Lambda')$ pertains to which particular electronic transition (band) $\Lambda''_n \to \Lambda'_n$, one can write equation (11) as a single sum,

$$\kappa_{tot}(\nu,T) = \frac{1}{\sqrt{k_B T}}\sum_i \exp\left(-\tfrac{E''_i}{k_B T}\right)\mathrm{A}_i\delta\left(\nu-\nu^{(i)}_{tr}\right), \quad (12)$$

where now the index i numbers all pairs $(v''_i, \Lambda''_i) \to (v'_i, \Lambda'_i)$ contributing to the total spectrum. The order of the terms in (12) is irrelevant in principle, but for computational convenience we order them according to decreasing values of transition frequencies $\nu^{(i)}_{tr}$.

In the calculation we took into account about 10^7 vibrational transitions, yet the computing time was 6–60 s only, depending on the temperature of the cesium vapor.

Equation (12) is applicable over a broad spectral range, except for the narow neighbourhoods of atomic spectral lines.

2.2 Thermal emission

The thermal emission from a uniform emitting layer, of thickness L and with the atomic number density $N_a = N$, given by the second term on the right-hand side of equation (5), is characterized by the spectral radiance $I(\nu,T)$ (in units of erg s^{-1} sr^{-1} cm^{-2} Hz^{-1}). In the LTE approximation it is simply related to the reduced absorption coefficient $\kappa(\nu,T)$ only, via Kirchhoff's law of thermal radiation, as

$$I(\nu,T) = \frac{2h\nu^3}{c^2}\frac{1-e^{-N^2 L\kappa(\nu,T)[1-\exp(-h\nu/k_B T)]}}{e^{h\nu/k_B T}-1}. \quad (13)$$

For an optically thin medium, $N^2 L\,\kappa(\nu,T) \ll 1$, or, more generally, if $\alpha_\nu L \ll 1$, the above expression simplifies to

$$I(\nu,T) = \frac{2h\nu^3}{c^2}N^2 L e^{-\frac{h\nu}{k_B T}}\kappa(\nu,T). \quad (14)$$

Whenever one can neglect the stimulated emission, i.e. if $h\nu/k_B T \gg 1$, equation (13) simplifies to

$$I(\nu,T) = \frac{2h\nu^3}{c^2}e^{-\frac{h\nu}{k_B T}}\left(1-e^{-N^2 L\kappa(\nu,T)}\right). \quad (15)$$

3 Results

The recent high-quality ab initio calculation [7] is the only source available in the literature which offers a complete theoretical input, i.e. both the adiabatic potential-energy curves and all electronic transition dipole moments required. Figure 1 shows the Hund's case (c) Cs_2 electronic potential-energy curves pertaining to the asymptotes $6s\ ^2S_{1/2} + 6s\ ^2S_{1/2}$, $6s\ ^2S_{1/2} + 6p\ ^2P_{1/2,3/2}$, and

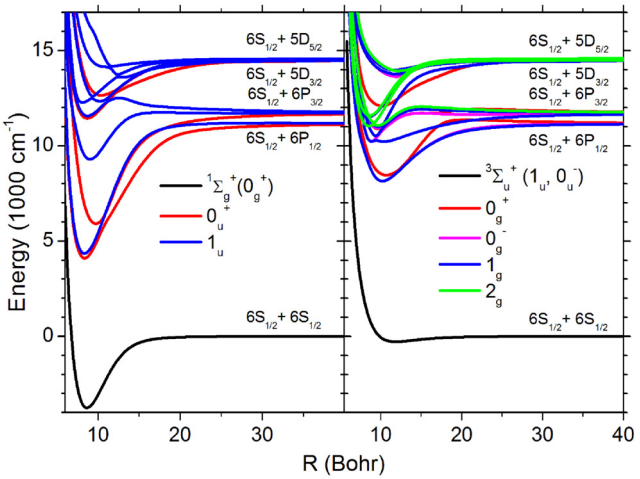

Fig. 1. Hund's case (c) adiabatic potential-energy curves of the Cs_2 molecule for the singlet (left) and triplet (right) electronic states [7], relevant for this study.

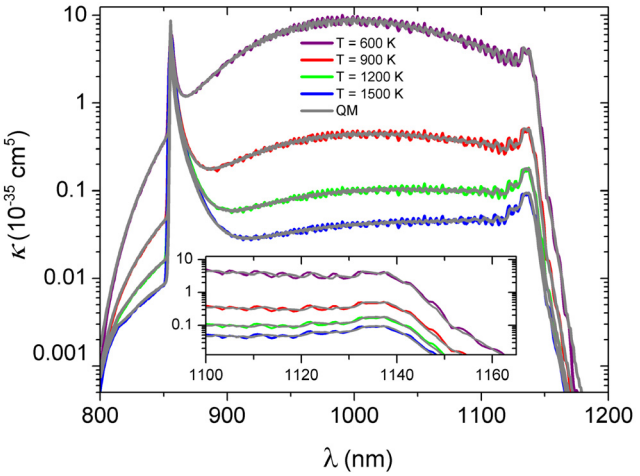

Fig. 2. Comparison of the SQA and QM calculations of the A–X band contribution to the reduced absorption coefficient of Cs_2 for four different temperatures. In the inset we show the expanded view of the spectrum in the range of 1100–1165 nm (the ordinates of the curves decrease in order of increasing temperatures).

$6s\ ^2S_{1/2} + 5d\ ^2D_{3/2,5/2}$. (The corresponding transition dipole moments are displayed in the original paper [7]).

We compared our SQA simulations of κ_ν for cesium vapor with the fully QM calculations and found better agreement for Cs_2 than for K_2. As an example, in Figure 2 we present the comparison of the SQA and QM calculations of the A–X band contribution to the reduced absorption coefficient of Cs_2 for four different temperatures. Since the curves in this comparison are difficult to discern, in the inset we show the expanded view of the spectrum in the range of 1100–1165 nm. As the found agreement is so good, further on we show only the results of the SQA.

The reduced absorption coefficients are displayed in Figure 3 for a range of temperatures. They can be compared to the wide-range spectra observed for example in references [12,13]. Benedict et al. [12] observed spectra over the wavelength range of 800–1300 nm, taken from 182 °C to 325 °C. Vdović et al. [13] presented the visible absorption spectra (615–915 nm) of cesium vapor in the 570–870 K temperature range. In our simulation all the salient spectral features are well reproduced: A–X, B–X, C–X, and D–X molecular bands (here we use traditional spectrosopic labels X, A, B,... and a, b, c,... based on the Hund's case (a) notation) as well as the quasistatic wings of Cs atomic lines (the first resonance doublet $6s\ ^2S_{1/2} + 6p\ ^2P_{1/2,3/2}$ and quadrupole lines $6s\ ^2S_{1/2} + 5d\ ^2D_{3/2,5/2}$). The dip in the absorption spectrum around 1150 nm reflects the spin-orbit coupling between the A (singlet) and b (triplet) states [14]. The A ($^1\Sigma_u^+$) and b ($^3\Pi_u$) electronic states cross each other, resulting in an avoided crossing in the corresponding 0_u^+ curves (see Fig. 1). The spin-orbit mixing results in a drastic change in the transition dipole moments. In the Hund's case (c) picture, the transition dipole moment from the X state towards the upper of these two 0_u^+ states (with a $^1\Sigma_u^+$ character at short distance) suddenly drops down beyond the crossing point, while the transition towards the lower 0_u^+ state (with a $^3\Pi_u$ character at short distances) "takes over" the intensity. The prominent features beyond the dip originate from the lower 0_u^+ state. The triplet diffuse band around 700 nm, located close to the short-wavelength end of the B–X band, originates in the transition from the lowest triplet state to the second $^3\Pi_g$ state which exhibits a peculiar configuration interaction with the first excited ionic state of the same symmetry [15]. There is also a very distinct satellite band at 875 nm, located between the two resonance lines of cesium, stemming from the Cs_2 $0_g^+(6s\ ^2S_{1/2} + 6p\ ^2P_{1/2})$ state [16]. However, some finer details (as, for example, the genuine inner-wing satellites [17]) are hardly seen in this wide-range spectral presentation.

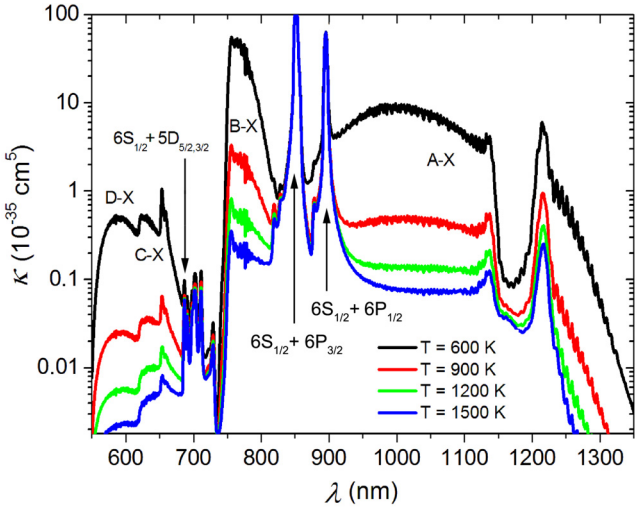

Fig. 3. The reduced absorption coefficient $\kappa = k/N^2$ for four different temperatures (the ordinates of the curves decrease in order of increasing temperatures).

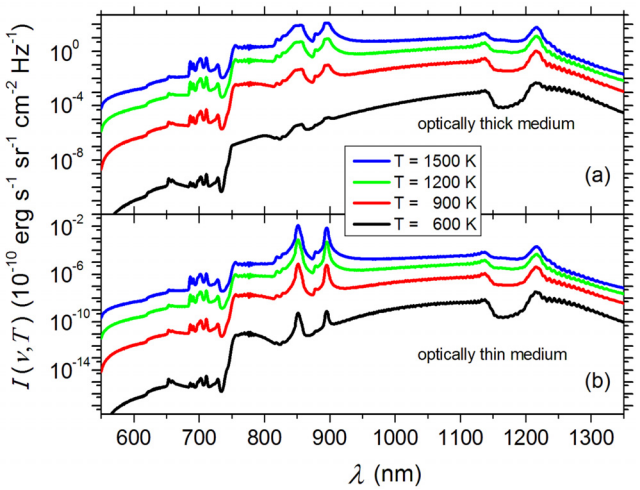

Fig. 4. Spectral radiance $I(\nu,T)$ of the thermal emission of an (a) optically thick medium ($\kappa N^2 L \gg 1$), with $N^2 L = 3 \times 10^{34}$ cm^{-5}, and (b) optically thin medium ($\kappa N^2 L \ll 1$), with $N^2 L = 10^{29}$ cm^{-5} (the ordinates of the curves increase in order of increasing temperatures).

Once the reduced absorption coefficient is known, and under the assumption that the LTE approximation holds, the spectral radiance $I_\nu(L)$ for the case of thermal *emission* can be obtained in a simple way, via equation (13). In Figure 4a we present the calculated spectral radiance $I(\nu,T)$ of the thermal emission of an optically thick medium ($\kappa N^2 L \gg 1$), with $N^2 L = 3 \times 10^{34}$ cm^{-5}, for a range of temperatures. In the regions around the centers of the first resonance doublet lines the spectral radiance reaches the plateau defined by the Planck curve $B_\nu(T)$ (see Eqs. (5) and (15)). On the other hand, all molecular features are still visible and their temperature dependence may be used for diagnostic purposes. For comparison, the spectral radiance of an optically thin medium ($\kappa N^2 L \ll 1$), with $N^2 L = 10^{29}$ cm^{-5}, is shown in Figure 4b. It bears basically the same information as the absorption coefficient itself, as is plain from equation (14).

4 Concluding remarks

In summary, we calculated the reduced absorption coefficient of dense cesium vapor at high temperatures (600–1500 K) for the red and near-infrared region (600–1300 nm), using a novel time-efficient "semiquantum" approximation (SQA). In our numerical simulation we took into account as many as 11 singlet and 19 triplet electronic transitions that contribute to the absorption spectrum in this region, handling about 10^7 vibrational transitions, yet the computing time was 6–60 s only, depending on the temperature. The comparison with fully QM calculations shows very good agreement, better for Cs_2 than for K_2, so that in certain situations/applications (e.g., no high-resolution spectrum required) one does not need the full QM calculation at all. The SQA thus gives a fairly accurate spectrum in a reasonably short time, which is very convenient indeed for *modelling* spectra of diatomic molecules. The consumption of computer time for the fully QM calculations (without the SQA "shortcut") is greater by up to four orders of magnitude, which might prove quite an impediment when it comes to practical applications like diagnostics and modelling, which require speed.

Assuming the validity of the local thermodynamic equilibrium (LTE) approximation, the spectral radiance $I_\nu(L)$ for the case of thermal emission can be expressed in terms of the reduced absorption coefficient only, via Kirchhoff's law of thermal radiation.

The overall features of the Cs_2 spectra are well reproduced in our SQA simulation. Also, these simulations, as well as those for K_2, exhibit desirable temperature sensitivity, which supports our expectations that the SQA numerical simulation of the spectrum can be a very efficient tool for the diagnostics of hot and dense dimer vapors. It also enables modelling of dense alkali vapor light sources.

This work was supported by the Croatian Science Foundation (HRZZ) under the project No. 2753 and, in its earlier phase, by the Ministry of Science, Education, and Sports of the Republic of Croatia under the project No. 035-0352851-3213. We are greatful to Vlasta Horvatić for her help in bringing the figures into their final form. R. B. thanks Goran Gatalica for his assistance in preparing some of the input data.

References

1. R. Beuc, M. Movre, B. Horvatić, Eur. Phys. J. D **68**, 59 (2014)
2. C. Vadla, R. Beuc, V. Horvatic, M. Movre, A. Quentmeier, K. Niemax, Eur. Phys. J. D **37**, 37 (2006)
3. W.C. Stwalley, M.E. Koch, Opt. Eng. **19**, 191071 (1980)
4. A. Zukauskas, M.S. Shur, R. Gaska, *Introduction to Solid State Lighting* (John Wiley & Sons, New York, 2002)
5. P. Flesch, *Light and Light Sources: High-Intensity Discharge Lamps* (Springer, Berlin-Heidelberg, 2006)
6. M. Rakić, G. Pichler, Opt. Commun. **284**, 2881 (2011)
7. A.R. Allouche, M. Aubert-Frécon, J. Chem. Phys. **136**, 114302 (2012)
8. A. Thorne, U. Litzén, S. Johansson, *Spectrophysics – Principles and Applications* (Springer Verlag, Berlin-New York-Tokio, 1999)
9. H.R. Griem, *Principles of Plasma Spectroscopy* (Cambridge University Press, Cambridge, 1997)
10. F.G. Baksht, V.F. Lapshin, Plasma Phys. Rep. **38**, 1078 (2012)
11. V. Horvatic, S. Müller, D. Veza, C. Vadla, J. Franzke, Anal. Chem. **86**, 857 (2014)
12. R.P. Benedict, D.L. Drummond, L.A. Schlie, J. Chem. Phys. **66**, 4600 (1977)
13. S. Vdović, D. Sarkisyan, G. Pichler, Opt. Commun. **268**, 58 (2006)
14. R. Beuc, M. Movre, V. Horvatic, C. Vadla, O. Dulieu, M. Aymar, Phys. Rev. A **75**, 032512 (2007)
15. G. Pichler, S. Milošević, D. Veža, R. Beuc, J. Phys. B **16**, 4619 (1983)
16. R. Beuc, H. Skenderović, T. Ban, D. Veža, G. Pichler, W. Meyer, Eur. Phys. J. D **15**, 209 (2001)
17. D. Veža, M. Movre, G. Pichler, J. Phys. B **13**, 3605 (1980)